JOURNAL OF AGRICULTURAL AND FOOD CHEMISTRY
ARTICLE

J. Agric. Food Chem. 2009, 57, 6899–6907 6899
DOI:10.1021/jf9019322

Comparison of Gas Chromatography-Coupled Time-of-Flight Mass Spectrometry and ^{1}H Nuclear Magnetic Resonance Spectroscopy Metabolite Identification in White Wines from a Sensory Study Investigating Wine Body

Kirsten Skogerson,[†] Ron Runnebaum,[‡,∥] Gert Wohlgemuth,[†] Jeffrey de Ropp,[§] Hildegarde Heymann,[‡] and Oliver Fiehn*,[†]

[†]Genome Center, University of California, 451 Health Sciences Drive, Davis, California 95616, [‡]Department of Viticulture and Enology, University of California, One Shields Avenue, Davis, California 95616, and [§]NMR Facility, University of California, Davis, California 95616. [∥] Current address: Department of Chemical Engineering, University of California, One Shields Avenue, Davis, CA 95616

Metabolite profiles of white wines, including Chardonnay, Pinot gris, Riesling, Sauvignon blanc, and Viognier varieties, were determined using both gas chromatography-coupled time-of-flight mass spectrometry (GC-TOF-MS) and proton nuclear magnetic resonance spectroscopy (^{1}H NMR). A total of 108 metabolites were identified by GC-TOF-MS, and 51 metabolites were identified by ^{1}H NMR; the majority of metabolites identified include the most abundant compounds found in wine (ethanol, glycerol, sugars, organic acids, and amino acids). Compositional differences in these wines correlating to the wine sensory property "body", or viscous mouthfeel, as scored by a trained panel were identified using partial least-squares (PLS) regression. Independently calculated GC-TOF-MS and NMR-based PLS models demonstrate potential for predictive models to replace expensive, time-consuming sensory panels. At the modeling stage, correlations between the measured and predicted values have coefficients of determination of 0.83 and 0.75 for GC-TOF-MS and ^{1}H NMR, respectively. Additionally, the MS- and NMR-based models present new insights into the chemical basis for wine mouthfeel properties.

KEYWORDS: Metabolite profiling; wine body; mouthfeel; GC-TOF-MS; NMR; sensory modeling

INTRODUCTION

One key sensory attribute of any wine is its body, or viscous mouthfeel properties. Perceived body makes an important contribution to the overall mouthfeel (tactile) perception of a wine along with other mouthfeel sensations such as astringency, heat, and carbonation (*1*); it is routinely described using terms ranging from watery (absence of body) to light-, medium-, or full-bodied. For white table wines, which lack the tannins responsible for red wine astringency and the carbonation of sparkling wines, perceived body is the major tactile sensation. Despite the importance of body in defining and differentiating styles and qualities of wines, its precise origins remain unclear. Prior work on the impact of rheological properties on wine body has led to a partial understanding of a few chemical constituents influencing this sensory quality (*2*−*6*); however, a more comprehensive understanding of the chemical and physical properties related to wine body remains to be determined. Ultimately, once compounds are identified, viticultural and enological practices that influence their concentrations can be elucidated and subsequently implemented to target the desired sensory characteristics.

*To whom correspondence should be addressed. Telephone: (530) 754-8258. Fax: (530) 754-9658. E-mail: ofiehn@ucdavis.edu.

Human senses are composed in the brain by pattern recognition of different magnitudes of signals received at peripheral receptors (*7*). Consequently, "mouthfeel" will not be able to be explained by a single variable, but rather by a combination of variables. Wine is a complex mixture, and global chemical profiling techniques, such as metabolite profiling, could be employed to expand the list of chemical constituents routinely measured in wine samples.

Gas chromatography-coupled mass spectrometry (GC−MS) and nuclear magnetic resonance spectroscopy (NMR) are the two most frequently used tools for metabolite profiling; both generate high-density, diverse chemical data sets, each with specific advantages and drawbacks (*8*). NMR has been employed in the characterization of both grapes and wines for purposes of authentication and classification (*9*−*11*) and in investigation of the chemical basis for the concept *terroir* (*12*). Recently, researchers have demonstrated the potential for ^{1}H NMR applications in monitoring primary and secondary fermentations (*13*). GC−MS has been employed primarily for analyses of aroma compounds and in the detection of spoilage compounds (*14*−*16*). At present, no study reports independently curated metabolite lists for wines using MS and NMR technologies or compares experimental conclusions drawn from independently generated data for the

Published on Web 07/09/2009

purpose of a direct comparison of the two technologies with regard to wine analysis.

Partial least-squares (PLS) regression has been successfully used in food product analysis to interpret the results obtained by sensory analysis (*17*−*20*) and allows for correlations to be established between sensory attributes and other types of variables, such as metabolite data. Additionally, PLS regression can be used to construct models that allow sensory characteristics to be predicted from simpler laboratory measures. Analysis of the wine metabolite data and sensory panel assessments using multivariate statistical methods could allow for the identification of a suite of compounds that ultimately define the sensation of wine body.

This study compares GC-TOF-MS- and ^{1}H NMR-based metabolite profiles of white wines, including Chardonnay, Pinot gris, Riesling, Sauvignon blanc, and Viognier varieties. The goal of this work is to identify compositional differences in these wines which correlate to the wine sensory property "body", or viscous mouthfeel, using multivariate statistical methods. The feasibility of developing a robust predictive model as a time- and cost-effective alternative to obtaining sensory data is also explored.

MATERIALS AND METHODS

Reagents. Reference standards used in creating the GC-TOF-MS library and all fatty acid methyl esters were purchased from Sigma (St. Louis, MO), Fluka (Sigma-Aldrich), or Aldrich (Milwaukee, WI). The reference standard for inulobiose was a gift from A. van Laere and W. van den Ende (Katholieke University, Leuven, Belgium). Pyridine and *N*-methyl-*N*-trimethylsilyltrifluoroacetamide with 1% trimethylchlorosilane (MSTFA + 1% TMCS) were obtained through Thermo Scientific (Rockford, IL). D_2O (99.9%) was provided by Cambridge Isotope Laboratories, Inc. (Andover, MA). Methoxyamine hydrochloride and sodium 3-trimethylsilyl-2,2,3,3-d_4-propionate (TMSP) were purchased from Sigma-Aldrich.

Sample Preparation. Commercially available white wines ($n = 17$) representing six varieties, three vintages, and multiple winemaking regions were chosen for analysis and spanned an anecdotal range of wine body styles from light- to full-bodied (**Table 1**). Samples were prepared by reducing 1 mL of wine under vacuum (Vacufuge Concentrator, Eppendorf) by half to decrease both the ethanol and water content. The reduced-volume wine samples were then D_2O-exchanged twice with the addition of 500 μL of D_2O followed by another concentration step (i.e., the H_2O content of final samples was minimally 25%). Wines were never concentrated more than 2-fold to prevent the formation of insoluble precipitates.

GC-TOF-MS Samples. Samples were prepared for injection using a two-step methoximation−silylation protocol (*21*). Concentrated, dealcoholized D_2O-exchanged wine samples (1 μL) were dried under vacuum (Labconco CentriVap), and then 10 μL of methoxyamine hydrochloride (40 mg/mL pyridine) was added to the dried samples before they were agitated at 30 °C for 90 min. Following the addition of 90 μL of MSTFA + 1% TMCS, samples were agitated for an additional 30 min at 37 °C. A retention index marker mixture comprised of fatty acid methyl esters of C8, C9, C10, C12, C14, C16, C18, C20, C22, C24, C26, C28, and C30 linear chain lengths dissolved in chloroform at 0.8 mg/mL (C8−C16) or 0.4 mg/mL (C18−C30) was spiked into samples (2 μL). Samples were prepared in triplicate and injected twice for a total of six measurements per wine, which were averaged prior to statistical analysis.

Acquisition of GC-TOF-MS Data. GC-TOF analysis was performed on a 6890 gas chromatograph (Agilent Technologies) equipped with a CIS 4 temperature programmable injector and MPS2 multipurpose sampler (Gerstel) and interfaced with a Pegasus IV time-of-flight mass spectrometer (Leco). Automated injections and linear exchanges were performed by the MPS 2 instrument. Injections (0.5 μL) were performed in splitless mode (purge time of 25 s, purge flow rate of 40 mL/min). The injector was programmed at an initial temperature of 50 °C with a 0.0 min hold and then ramped up to a final temperature of 275 °C at a rate of 12 °C/s followed by a 3 min hold. Multibaffled glass linears were changed every 10 samples. Chromatographic separation was performed on a Rtx-5Sil MS column with a 10 m integrated guard column [95% dimethyl/5% diphenyl polysiloxane film; 30 m × 0.25 mm (inside diameter) × 0.25 μm d.f. (Restek)]. The GC oven temperature program was as follows: initial temperature of 50 °C with a 1 min hold followed by a 20 °C/min ramp up to 330 °C with a 5 min hold. The carrier gas (99.9999% He) was kept at a constant flow of 1 mL/min. The transfer line temperature between the gas chromatograph and mass spectrometer was 280 °C. Following a 335 s solvent delay, mass spectra were acquired at 20 scans/s with a mass range of m/z 85−500. The detector voltage was 1800 V and the electron energy 70 V. The ion source temperature was set at 250 °C.

Table 1. List of Wines Studied

grape variety	sample ID	vintage	region
Chardonnay	CH01	2003	Napa Valley, CA
	CH02	2003	Napa Valley, CA
	CH03	2004	Napa Valley, CA
	CH04	2003	Monterey, CA
	CH05	2003	Napa Valley, CA
	CH06	2004	Southeast Australia
Pinot gris	PG01	2003	Oregon
	PG02	2004	Napa Valley, CA
Riesling	R01	2004	Napa Valley, CA
	R02	2004	New York
Sauvignon blanc	SB01	2001	Lake County, CA
	SB02	2004	Napa Valley, CA
	SB03	2004	Napa Valley, CA
	SB04	2004	Napa Valley, CA
Viognier	V01	2004	Yolo County, CA
	V02	2004	Napa Valley, CA
white wine	WW01	2004	Napa Valley, CA

GC-TOF Data Processing. Peak detection and mass spectrum deconvolution were performed with Leco ChromaTOF software (version 2.32). Automatic alignment and compound identification using a mass spectral/retention index library were performed using the BinBase algorithm (*22*). BinBase assigns and tracks both identified compounds and unknown compounds using the retention index and mass spectrum as the two most important identification criteria. All BinBase database entries are matched against the Fiehn mass spectral library, which was generated from pure standards using identical instrument parameters outlined above and contains 712 unique metabolites. Additional confidence criteria are provided by mass spectral metadata, including unique ions, apex ions, peak purity, and signal:noise ratios as specified in data preprocessing. Tabulated data were normalized to total sum intensities of the 108 identified metabolites for each sample. The resulting data were multiplied by a constant factor to obtain values on scale with original values. All statistics were determined for the normalized data.

Acquisition of NMR Data. Prior to analysis, NMR samples were pH adjusted to 6.0 ± 0.06 with the addition of 1 M NaOH prepared in D_2O. All NMR spectra were recorded on a Bruker Avance 600 spectrometer with XWINNMR (version 3.1) operated at 600.02 MHz for ^{1}H and 150.87 MHz for ^{13}C. All data were collected at 298 K and referenced to the internal standard sodium 3-(trimethylsilyl)-2,2,3,3-d_4-propionate (TMSP, 1 mM) at a 0.00 ppm chemical shift for both proton and carbon dimensions.

One-dimensional (1D) ^{1}H NMR spectra were recorded using a one-pulse sequence with residual water presaturation. For each sample, 64 transients were collected using a 90° pulse into 32768 data points with a spectral width of 9.6 kHz. The pulse sequence recycle time was 3.7 s, and the total acquisition time was 5 min. Data sets were zero-filled to 32768 points, and an exponential line broadening of 0.3 Hz was applied before Fourier transformation. The resulting spectra were phase corrected manually and baseline corrected using an automated quintic polynomial function.

In addition, two-dimensional (2D) ^{1}H−^{1}H COSY and ^{1}H−^{13}C HSQC NMR experiments were performed with the same sample to aid in the assignment of metabolites. ^{1}H−^{1}H magnitude-mode COSY spectra were collected with 2048 points in t_1 and 256 points in t_2 over a bandwidth of 10 ppm, with 16 scans per t_1 value. Spectra were processed with 0°-shifted sine-squared apodization in both dimensions and zero filling in t_1 to yield a transformed 2D data set of 1024 × 1024 points. ^{1}H−^{13}C HSQC spectra

were collected in the echo−antiecho phase-selective mode with 2048 points in t_1 and 256 points in t_2 over a bandwidth of 12 ppm in ^{1}H and 170 ppm in ^{13}C, with 16 scans per t_1 value. HSQC spectra were processed with 90°-shifted sine-squared apodization, phase correction in both dimensions, and zero filling in t_1 to yield a transformed 2D data set of 1024×2048 points. The measurement time was 116 min for COSY and 134 min for HSQC.

NMR Data Processing. Metabolite identification and quantification were performed on one-dimensional spectra using the 600 MHz library from the Chenomx NMR software suite (version 5.0). Assignments were confirmed with two-dimensional spectra and comparison to published values (*23*). In preparation for multivariate statistical analysis, each spectrum was segmented into 0.005 ppm bins between 0.0 and 10.0 ppm with bins from 4.70 to 5.15 ppm excluded from all spectra to remove any variations in the presaturation of the water resonance. The total area of each spectrum was normalized to 1. Integration into bins and normalization were performed in Chenomx.

Sensory Assessment. Details of the sensory portion of this study can be found elsewhere (*6*). Briefly, a panel of 10 trained assessors evaluated the wines using descriptive analysis techniques. Wines were presented in random order (randomized block design) under red light to prevent any color-based bias. Panelists evaluated each of the 17 wines in triplicate. The intensity of the mouthfeel viscosity was rated on a 10 cm unstructured line scale anchored at the extremes by high and low markers. The mean of the scores was calculated and used for statistical analysis. Fisher's protected least significant difference was used ($\alpha = 0.05$, double-sided) to compare the means.

Statistical Analysis. Statistical analyses were performed on GC-TOF-MS metabolite data and the ^{1}H NMR bins using Statistica version 7.1. Prior to analysis, the 17 wines were divided into three groups representing light-bodied ($n = 6$), medium-bodied ($n = 5$), and full-bodied wines ($n = 6$) based on panel ranking. Univariate statistical analysis was performed by breakdown and one-way ANOVA; F statistics and P values were generated for all metabolites. Data distributions were displayed by box−whisker plots, giving the arithmetic mean value for each category and the standard error as box and whiskers for 1.96 times the category standard deviation to indicate the 95% confidence intervals, assuming normal distributions.

Partial least-squares (PLS) regression was used to investigate relationships between wine mouthfeel scores and normalized GC-TOF-MS metabolites (108 identified and 305 unidentified compounds) or binned NMR data. Data analysis was performed using the Unscrambler software package (version 9.0, CAMO ASA). All data were standardized prior to calculations (weighting option = 1/SDEV), and model evaluations were based on the full cross validation procedure. Significant variables were identified on the basis of a cross validation/jackknifing procedure, and variables that were deemed unreliable were eliminated to simplify the model (*24*). The quality of the model's predictive ability was assessed by the percent variance of the Y-variables explained by the X-variables, correlation coefficients between measured and predicted variables, the root-mean-square error of calibration (RMSEC), which is a measure of the average modeling error, and the root-mean-square error of prediction (RMSEP) which provides a measure of the model's ability to predict a mouthfeel viscosity score on a new sample on the basis of the cross validation procedure.

RESULTS

GC-TOF-MS Metabolite Profiling. Fully automated annotation of GC-TOF-MS data by the BinBase algorithm reliably detected more than 400 metabolites in all wine samples. Of these, 108 are identified by retention index-based mass spectral libraries and include amino acids, organic acids, sugars, sugar alcohols, sugar acids, and fatty acids as well other metabolites (**Table 2**). The remaining 305 are unique structurally unidentified metabolites consistently detected in the samples. Full metabolite lists for the wines are available through the SetupX public database (http://fiehnlab.ucdavis.edu:8080/m1/main_public.jsp). Spectra of unidentified compounds, their presence in other organisms, lists of chemically similar compounds, and further information can be found at http://eros.fiehnlab.ucdavis.edu:8080/binbase-compound/. A sample GC-TOF-MS chromatogram is provided in the Supporting Information.

Table 2. Overview of Metabolites Found in White Wine by GC-TOF-MS and ^{1}H NMR

metabolite	GC-TOF-MS	NMR	metabolites common to both data sets
amino acids[a]	28	21	20
organic acids[b]	22	12	9
sugars	16	6	6
sugar alcohols	16	3	3
sugar acids	6	1	1
fatty acids	10	0	0
amines	5	2	2
miscellaneous[c]	5	6	2
total	**108**	**51**	**43**

[a] Cysteine, GABA, glycine, homoserine, pipecolic acid, and 4-hydroxyproline detected by GC-TOF-MS but not NMR, saccharopine and suberylglycine detected by GC-TOF-MS but not in the NMR library, and *N*-acetyltyrosine detected by NMR but not in the GC-TOF-MS library. [b] α-Ketoglutarate and threonic acid detected by GC-TOF-MS but not NMR, fumaric acid detected by NMR but not GC-TOF-MS, 2-furoate and acetate detected by NMR but not in the GC-TOF-MS library, and 11 additional organic acids detected by GC-TOF-MS but not in the NMR library. [c] Xanthine detected by GC-TOF-MS but not NMR, trigonelline detected by NMR but not GC-TOF-MS, guanine and nicotianamine detected by GC-TOF-MS but not in the NMR library, and acetaldehyde, ethanol, and formate detected by NMR but not in the GC-TOF-MS library.

^{1}H NMR Metabolite Profiling. ^{1}H NMR spectral assignments yielded approximately half the number of metabolites identified by GC-TOF-MS (51 and 108, respectively). Portions of each wine spectrum remained unassigned due to spectral overlap and Chenomx metabolite library limitations. The 51 metabolites that were assigned include amino acids, organic acids, sugars, and sugar alcohols, as well as other metabolites (**Table 2**). Full metabolite lists for the wines are available through the SetupX public database (http://fiehnlab.ucdavis.edu:8080/m1/main_public.jsp). A sample ^{1}H NMR spectrum is provided as Supporting Information.

GC-TOF-MS and NMR Metabolite Comparison. The majority of metabolites identified by both GC-TOF-MS and NMR include the most abundant compounds found in wine: ethanol, glycerol, sugars, organic acids, and amino acids. The greatest overlap between GC-TOF-MS and NMR metabolite profiles was seen for amino acids; 20 amino acids were common to both data sets (Ala, Arg, Asn, Asp, β-Ala, Glu, Ile, Leu, Lys, Met, Phe, Pro, Ser, Thr, Trp, Tyr, Val, citrulline, ornithine, and oxoproline). Several amino acids, including cysteine, GABA, glycine, homoserine, pipecolic acid, and 4-hydroxyproline, are present in both MS and NMR libraries and were detected by GC-TOF-MS but not by NMR. Saccharopine and suberylglycine, two additional amino acids identified by GC-TOF-MS, are not in the Chenomx library, and *N*-acetyltyrosine, which was identified in the NMR spectra, is not in the current GC-TOF-MS library.

Organic acid profiles also showed good overlap with nine amino acids common to both GC-TOF-MS and NMR data sets (2-hydroxyglutaric, benzoic, citric, isocitric, lactic, malic, maleic, and succinic acids and tartrates). Eleven of those detected by GC-TOF-MS are not in the NMR library (2-isopropylmalic, 2-ketoisocaproic, 3-hydroxy-3-methylglutaric, caffeic, *cis*-caffeic, citramalic, dehydroascorbic, indole-3-lactic, isothreonic, quinic, and shikimic acids), and two identified in the NMR spectra are not in the GC-TOF-MS library (2-furoate and acetate). Several organic acids represented in both libraries are only found in one data set or the other; fumarate is detected by only NMR, and threonate and α-ketoglutarate are detected by only GC-TOF-MS.

Sugars, sugar alcohols, and sugar acids are not well-represented in the Chenomx library; those identified by GC-TOF-MS

but not NMR are not present in the Chenomx library. Sugars and sugar derivatives identified by both technologies include fructose, fucose, galactose, glucose, ribose, xylose, glycerol, mannitol, myo-inositol, and glyceric acid. The Chenomx library does not contain fatty acids, and therefore, none were assigned in the NMR data set. Those identified by GC-TOF-MS include arachidic, behenic, butylstearic, heptadecanoic, lauric, oleic, palmitic, pelargonic, and stearic acids, as well as the fatty alcohol octadecanol.

Table 3. Mean Perceived Viscous Mouthfeel Ratings and Assigned Wine Body Classification Used for ANOVA

sample	mouthfeel viscosity score (panel mean)[a]	wine body classification
CH03	3.21 a	high
CH05	2.91 ab	high
CH02	2.85 abc	high
R02	2.63 bcd	high
CH01	2.57 bcd	high
CH04	2.55 bcd	high
CH06	2.46 bcde	medium
R01	2.44 bcde	medium
V01	2.42 bcde	medium
SB03	2.33 cde	medium
V02	2.32 cde	medium
PG02	2.24 de	low
WW01	2.22 de	low
SB01	2.16 de	low
PG01	2.13 de	low
SB04	2.12 de	low
SB02	1.97 e	low

[a] Wines with the same letter are not significantly different at $\alpha = 0.05$.

In summary, a total of 43 metabolites are found in both GC-TOF-MS and NMR data sets. Of the 108 compounds identified by GC-TOF-NMR, 54 are not in the NMR library, which prevented their assignment. In 13 cases, the metabolite was present in both libraries but was either not detected by GC-TOF-MS (two metabolites) or not detected by NMR (11 metabolites). The eight compounds detected by NMR but not GC-TOF-MS include fumarate and trigonelline (present in both libraries), as well as acetaldehyde, acetate, ethanol, formate, 2-fuorate, and methanol (not in the GC-TOF-MS library). These six compounds are not found in the GC-TOF-MS library because they elute in the proximity of the methoximation−silylation reagents during the solvent delay.

Wine Sensory Assessments. Results from the panel's scoring of perceived viscous mouthfeel showed significant differences among the 17 wines (**Table 3**). Mean scores ranged from 1.97 for one of the Sauvignon blanc wines (SB02) to 3.21 for one of the Chardonnay wines (CH03). A Fisher's protected least significant difference of 0.5791 (df = 16, $\alpha = 0.05$, double-sided) between viscosity scores indicates a statistically significant difference. Wines were classified in three groups (high, medium, and low) on the basis of the mean mouthfeel viscosity score determined by the panel for univariate statistical analysis. Detailed results from the complete sensory assessment of the wines are discussed elsewhere (*6*).

Analysis of Variance. Analysis of variance (ANOVA) identified significant differences among compounds in the three wine body classification groups (high, medium, and low). Of the 108 metabolites measured by GC-TOF-MS, 28 analytes showed significant differences between body classifications at the 95% level (**Table 4**). The significant metabolites include amino acids, fatty acids, organic acids, sugars, and sugar acids. In general, fatty

Table 4. One-Way ANOVA of the Variation of Mean Normalized Peak Heights of Metabolites Detected in White Wines by GC-TOF-MS among High-, Medium-, and Low-Wine Body Classification Groups[a]

metabolite[b]	high ($n = 6$)	medium ($n = 5$)	low ($n = 6$)	p[c]	PubChem CID
palmitic acid	8626	11577	18139	<0.0001	985
stearic acid	56824	73447	130003	<0.0001	5281
ribose	6026	6305	9210	<0.001	993
tartrate	395112	490648	681968	<0.001	875
2-ketoisocaproate	529	656	827	<0.001	70
octadecanol	807	1018	1384	0.002	8221
4-hydroxyproline	15945	10688	7706	0.002	825
myo-inositol	204703	387406	361549	0.004	892
maleate	242356	134687	107717	0.005	444266
sophorose	6176	13626	18195	0.006	92797
xylitol	1946	3816	3629	0.006	6912
dehydroascorbate	9449	9154	21781	0.006	835
fucose	12163	15887	20149	0.008	17106
proline	2304004	1691843	1081451	0.015	614
inulobiose	1090	12358	1341	0.017	439552
oleic acid	251	283	437	0.019	965
isothreonic acid	3347	6253	3295	0.021	5282933
arachidic acid	1466	1808	2148	0.021	10467
cellobiose	13256	13422	42827	0.023	294
sorbitol	74624	137416	99570	0.025	5780
threitol	7231	17102	14502	0.028	169019
behenic acid	1987	2695	2811	0.029	8215
phenylalanine	20262	12571	17521	0.030	6140
lysine	56250	32069	49809	0.031	5962
valine	45825	32258	37548	0.032	6287
shikimic acid	52489	29200	26441	0.033	8742
citrulline	6614	12943	4956	0.042	833
2-isopropylmalate	3937	4655	7794	0.044	5280523

[a] Mean values for significant metabolites are listed together with p values. [b] All metabolites identified by retention index and mass spectral match with standards run under identical instrument conditions. [c] A p of <0.05 indicates a significant difference.

Table 5. One-Way ANOVA of the Variation of Mean Concentrations (millimolar) of Metabolites Detected in White Wine Samples by ^{1}H NMR among High-, Medium-, and Low-Wine Body Classification Groups[a]

metabolite[b]	high (n = 6)	medium (n = 5)	low (n = 6)	p[c]	PubChem CID
valine	0.33	0.19	0.18	0.001	6287
phenylalanine	0.23	0.13	0.13	0.001	6140
isoleucine	0.20	0.11	0.11	0.002	6306
tyrosine	0.17	0.11	0.08	0.003	6057
proline	15.75	9.42	4.59	0.003	145742
serine	1.91	1.70	0.96	0.009	5951
glutamate	2.19	1.56	0.84	0.011	33032
mannitol	2.25	1.58	1.16	0.011	6251
leucine	0.59	0.30	0.34	0.012	6106
benzoate	0.03	0.01	0.01	0.016	243
tryptophan	0.05	0.04	0.02	0.024	6305
malate	1.00	3.72	1.53	0.028	525
oxoproline	2.01	1.67	0.95	0.032	7405
maleate	0.02	0.01	0.01	0.033	444266
alanine	1.88	1.53	0.80	0.033	5950
2-furoate	0.05	0.03	0.02	0.037	6919
fumarate	<0.01	0.01	<0.01	0.038	444972
ethanol	0.76	0.60	0.55	0.045	702
myo-inositol	2.39	3.96	2.32	0.046	892
isocitrate	1.53	1.39	0.84	0.047	5318532
2-hydroxyglutarate	0.70	0.61	0.51	0.048	43
arginine	1.32	1.90	0.96	0.048	232
trigonelline	0.17	0.17	0.12	0.048	5570

[a] Mean values for significant metabolites are listed together with p values. [b] All NMR metabolite assignments are based on Chenomx software assignments and literature value and are, as such, tentative. [c] A p of <0.05 indicates a significant difference.

acids appear to have higher mean concentrations in the low-wine body classification group, while all other metabolite types showed positive, negative, and mixed trends. Significant differences were seen for 23 of the 53 Chenomx-assigned metabolites (**Table 5**). More than half of these are amino acids, and the majority of these had higher mean concentrations for the wines in the high-wine body classification group.

GC-TOF-MS PLS Model. Partial least-squares (PLS) regression analysis of the viscous mouthfeel scores and the GC-TOF-MS metabolite data indicates that 82% of the variation in perceived viscous mouthfeel can be explained by the first two dimensions (**Figure 1**). In the scores plot (**Figure 1A**), the wines appear on a continuum along the first dimension (73% variance explained) with lighter-bodied wines negatively loaded on PC1 and the fuller-bodies wines positively loaded. There is no obvious separation among the wines in the second dimension (9% variance explained). A total of 74% of the variation in the metabolite profiles is described by the model, with 65% explained in the first dimension and 9% explained in the second. The correlation loadings plot (**Figure 1B**) allows for the visualization of the relationship between the individual metabolites and wine body score; those metabolites on the right are positively correlated to the mouthfeel score, while those on the left are negatively correlated.

Both identified and unidentified metabolites are key variables in the model. Of the identified metabolites, proline is most strongly positively correlated (0.744) to viscous mouthfeel score (**Figure 1C**). Five unidentified compounds are also strongly correlated to mouthfeel score. The BinBase identifiers for these compounds and their correlation coefficients are 224909 (0.913), 200478 (0.909), 199232 (0.899), 225846 (0.821), and 213266 (0.700). The similarity of these five compounds to known library compounds suggests that these compounds are sugar alcohols or sugar acids (mass spectral similarity score of >700 with respect to library standards galactitol, sorbitol, and galactonic acid). Fatty acids palmitate (−0.942) (**Figure 1D**) and stearate (−0.908) are the most negatively correlated to viscous mouthfeel score along with six unidentified compounds. The BinBase identifiers for these compounds and their correlation coefficients are: 224521 (−0.982), 224791 (−0.978), 215355 (−0.974), 200427 (−0.967), 217841 (−0.966), and 224522 (−0.966). The similarity of these six compounds to known library compounds suggests these are amines or amino compounds (mass spectral similarity score of >700 with respect to library standards allantoin, putrescine, and aminomalonate). Results from two representative library searches for mass spectral similarity are shown in the Supporting Information (Figure S2).

Model statistics are summarized in **Table 6**. The predictive ability of the model at the calibration stage of model building yielded a coefficient of determination of 0.83, which decreased to 0.67 at the validation stage. At both calibration and validation stages of model building, the root-mean-square error values were below 0.2 unit on the mouthfeel rating scale (0.131 and 0.182, respectively), where the range of average mouthfeel viscosity scores was 1.24 and wines with scores differing by 0.5791 were significantly different (Fisher's protected LSD, $\alpha = 0.05$, double-sided).

^{1}H NMR PLS Model. PLS analysis of the viscous mouthfeel scores and the ^{1}H NMR binned data indicates that 79% of the variation in perceived viscous mouthfeel can be explained by the first two dimensions (**Figure 2**); 75% of the variation is explained in the first dimension and 4% in the second. In the scores plot (**Figure 2A**), the wines with the highest viscous mouthfeel score are positively loaded on PC1, and those with medium or low scores are intermixed and more negatively loaded on PC1. A total of 56% of the variation in the NMR spectral bins is described by the model, with 44% explained in the first dimension and 12% explained in the second. The correlation loadings plot (**Figure 2B**) shows the relationship between the individual spectral bins and wine mouthfeel score; those bins on the right are positively correlated to the mouthfeel score, while those on the left are negatively correlated.

Spectral regions positively correlated to viscous mouthfeel score with their correlation values and tentative compound assignments are as follows: 3.4075 (0.861, proline), 4.1225 (0.85, proline/lactate), 9.1025 (0.837, trigonelline), 9.1075 (0.816, trigonelline), 1.9175 (0.809, acetate), 4.1075 (0.799, proline/lactate), and 4.1275 (0.755, proline/lactate) (**Figure 2B**). Additional bins in the final model which also contain proline, lactate, and trigonelline resonances include 3.3925 (0.745, proline), 3.3975 (0.725, proline), 1.3375 (0.631, lactate), 1.3325 (0.726, lactate), and 8.8325 (0.667, trigonelline). A plot of wine proline concentrations determined by Chenomx shows trends similar to those of the GC-TOF-MS proline values and demonstrates some overlap between the two data sets (**Figure 2C**). Spectral regions negatively correlated to mouthfeel score with their correlation values and tentative compound assignments include 4.3275 (−0.863, tartrate/malate), 3.7725 (−0.865, glycerol), 4.3325 (−0.841, tartrate), 3.5425 (−0.803, glycerol), 3.5325 (−0.801, glycerol), 3.5625 (−0.777, glycerol), and 3.5525 (−0.745, glycerol) (**Figure 2B**). A detailed view of the NMR spectra averaged by mouthfeel grouping clearly shows increased peak height for those bins positively correlated and decreased peak height for those bins negatively correlated (**Figure 2D**).

Model statistics are summarized in **Table 6**. The predictive ability of the NMR model at the calibration stage of model building yielded a coefficient of determination of 0.75, which decreased to 0.66 at the validation stage. At the calibration and validation stages of model building, the root-mean-square error values were 0.156 and 0.182 score unit, respectively, where the range of average mouthfeel scores was 1.24 and wines with scores differing by 0.5791 were significantly different (Fisher's protected LSD, $\alpha = 0.05$, double-sided).

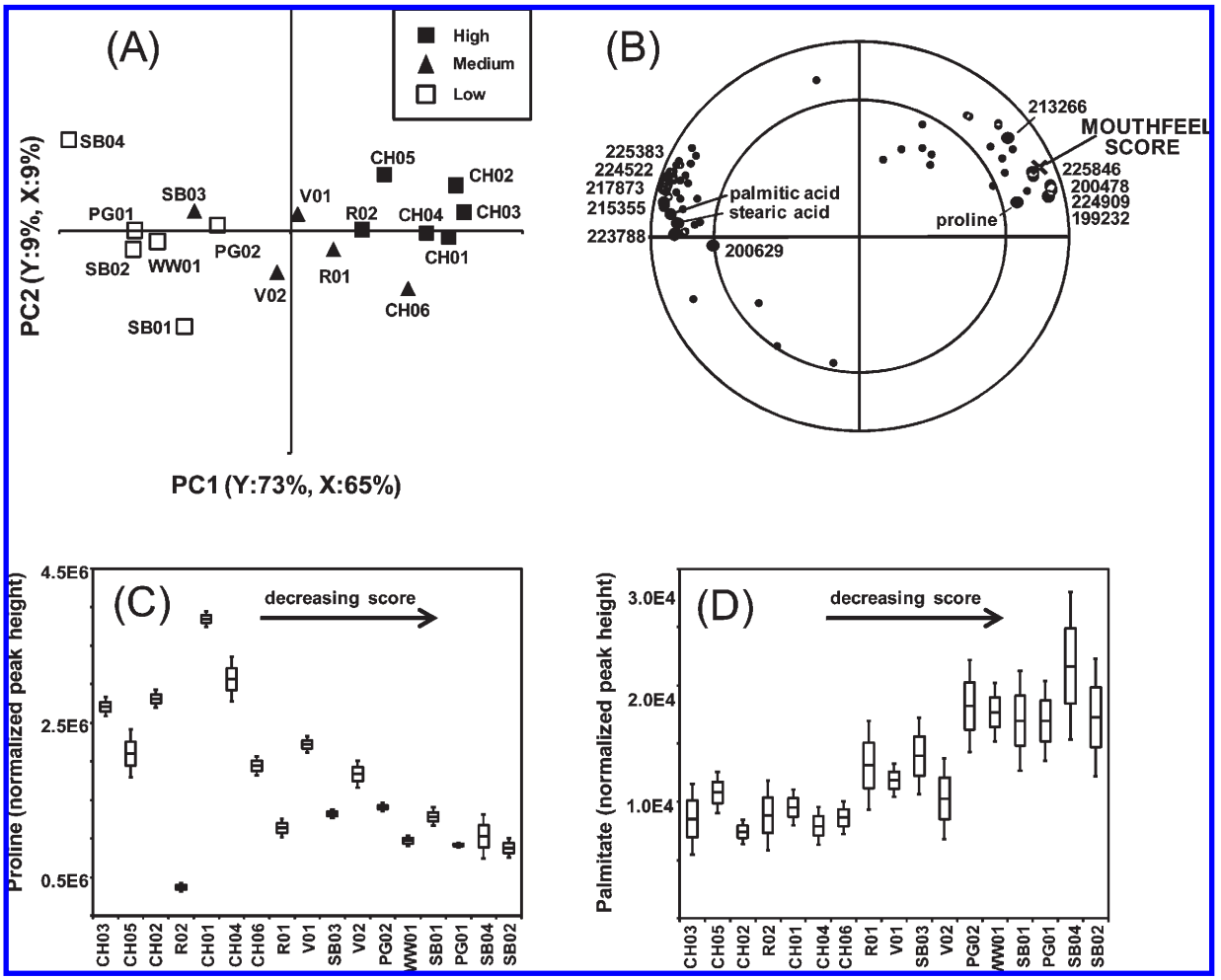

Figure 1. PLS scores plot (**A**) and correlation loadings plot (**B**) of viscous mouthfeel rating data (*Y*) and 71 GC-TOF-MS metabolites (*X*) used in model construction. The correlation loadings plot (**B**) aids in visualization of the relationship between the individual metabolites and wine mouthfeel score; those metabolites on the right are positively correlated to the mouthfeel score, while those on the left are negatively correlated. Both identified and unidentified metabolites are key variables in the model; those discussed in the text are marked with bold circles and labeled with either compound name or bin number (unidentified metabolites). Data distributions for metabolites proline (**C**) and palmitic acid (**D**) are displayed as box−whisker plots, giving the arithmetic mean value for each category and the standard error as box and whiskers for 1.96 times the category standard deviation. Wines are arranged on the *x*-axis in order of decreasing mouthfeel score.

DISCUSSION

Metabolite Identification by GC-TOF-MS and ^{1}H NMR. The 2-fold difference in the number of metabolites identified from GC-TOF-MS and NMR data sets (108 and 51, respectively) can be attributed to both the fundamental differences in the two technologies and the differences in the data annotation programs and their associated libraries. Detection limits are typically several orders of magnitude lower for MS than for NMR (picomolar and micromolar to nanomolar, respectively). Furthermore, the gas chromatography step performed prior to MS detection simplifies compound identification. While chromatography-coupled NMR systems are commercially available (e.g., LC-NMR), these instruments are not standard laboratory equipment. NMR-based metabolite analyses are typically performed on complex sample mixtures without any preseparation, and the identification of individual metabolites is complicated by many overlapping signals. In the absence of access to specialized LC-NMR equipment, one can conduct two-dimensional experiments to aid in compound assignment as we did in this study; however, this approach requires significant investment in both instrument time and data analysis time.

Global analysis of complex mixtures with the goal of identifying potentially minor differences requires robust data annotation tools. The GC-TOF-MS metabolite assignments in this study were performed by BinBase software and were fully automated. Fully automated NMR assignments were attempted with the full Chenomx library but yielded overfit data, and a semiautomated assignment strategy was employed. First, a sublibrary of metabolites identified by GC-TOF-MS analysis was created in Chenomx; then these metabolites were automatically assigned, and finally, manual correction of peak shifts and intensities was performed. Thus, NMR metabolite assignments by the software not only required knowledge of the compounds present but also required significant hands-on time for the manual correction of peak shifts and intensities. Library limitations also affected the number of metabolites assigned by the two methodologies. A comparison of the Fiehn and Chenomx libraries with the KEGG metabolite database (release 45.0) reveals that the Fiehn library contains 3 times the number of KEGG metabolites (695 of 712) compared to Chenomx (206 of 270).

In summary, GC-TOF-MS proved superior to NMR for the identification of white wine metabolites. The GC-TOF-MS metabolite list was more comprehensive, and assignments were

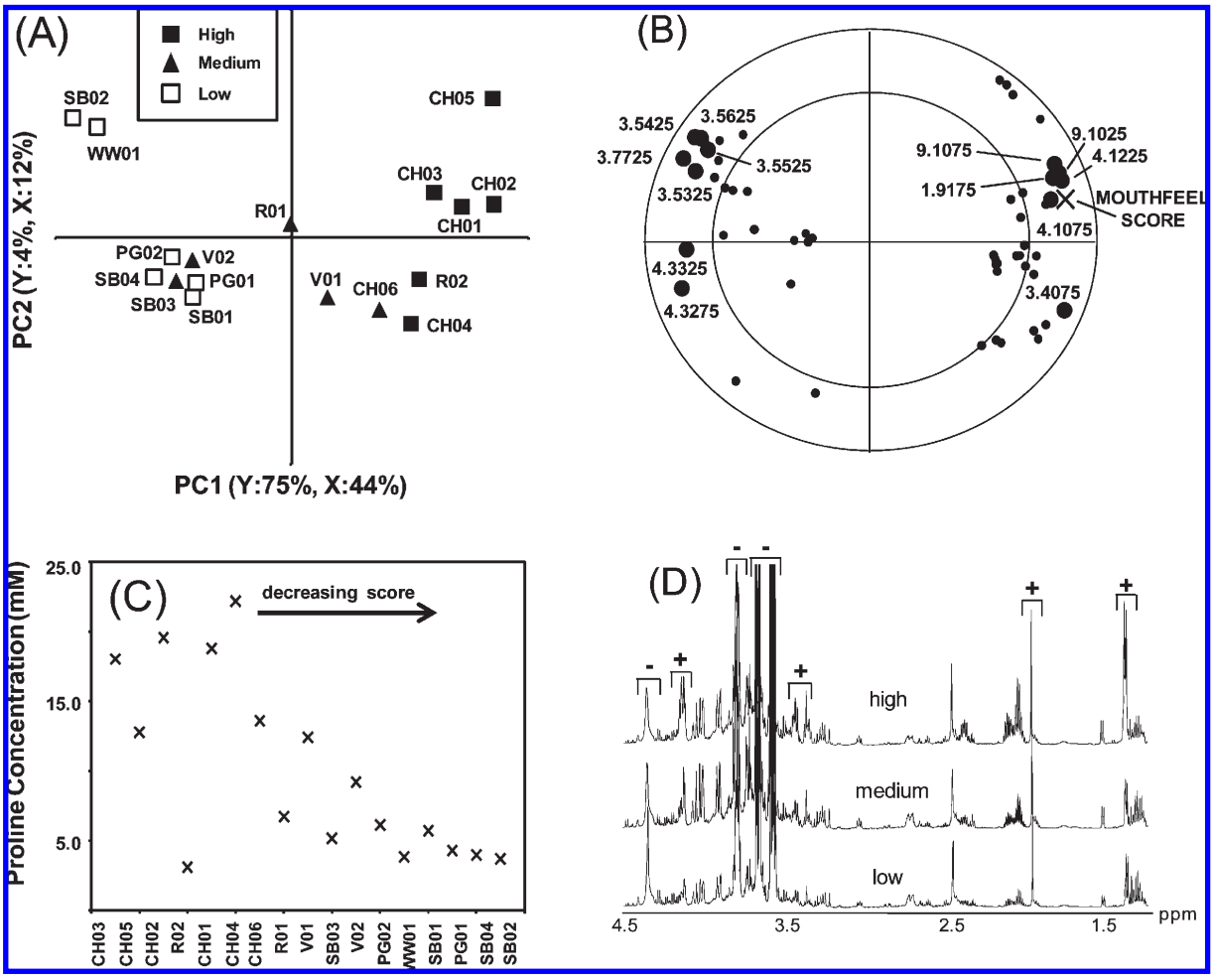

Figure 2. PLS scores plot (**A**) and correlation loadings plot (**B**) of viscous mouthfeel rating data (*Y*) and 54 NMR spectral bins (*X*) used in model construction. The correlation loadings plot (**B**) aids in visualization of the relationship between the NMR bins and wine mouthfeel score; those bins on the right are positively correlated to the mouthfeel score, while those on the left are negatively correlated. Key bins discussed in the text are marked with bold circles and labeled with the bin value (parts per million). Wine proline concentrations determined by the Chenomx software are plotted in panel **C** on the *Y*-axis in order of decreasing mouthfeel score. Averaged ^{1}H NMR spectra (**D**) for high-body ($n = 6$), medium-body ($n = 5$), and low-body ($n = 6$) mouthfeel wines with binned regions positively (+) and negatively (−) correlated to mouthfeel score are highlighted.

Table 6. Summary of Calibration and Validation Model Statistics for GC-TOF-MS and NMR Predictive Models

				calibration		validation	
	no. of significant components	no. of significant variables[a]	% *Y* explained	r^2	RMSEC[b]	r^2	RMSEP[c]
GC-TOF-MS	2	71	82	0.83	0.131	0.67	0.182
NMR	1	54	79	0.75	0.156	0.66	0.182

[a] Identified by a cross-validation/jack-knifing procedure (*19*). [b] Root-mean-square error of calibration; values expressed in mouthfeel score units. [c] Root-mean-square error of prediction as calculated by leave-one-out cross validation procedure; values expressed in mouthfeel score units.

complete in a fraction of the time required for the NMR data. NMR assignments required additional data collection for assignment confirmation; however, development of wine-specific compound libraries for NMR might reduce this time and increase the number of compounds identified. Ultimately, equipment availability frequently dictates the analytical methods used, and both GC-TOF-MS and NMR demonstrate the ability to generate substantial information regarding white wine metabolites.

GC-TOF-MS and NMR PLS Model Comparison. In this study, PLS regression was used to investigate the relationship between the metabolite data and the mouthfeel viscosity rating of 17 white wines. This approach identifies a linear combination of compounds that best model the viscous mouthfeel perception scored by the sensory panel. PLS models were built independently with either the GC-TOF-MS data or the NMR data. GC-TOF-MS models were constructed from the complete metabolite data set (identified and unidentified compounds). Analysis of the NMR data was performed using the standard method of spectral binning, which allowed for the inclusion of unassigned portions of the spectrum in the PLS solution.

Results from the PLS modeling suggest that both GC-TOF-MS and NMR models have the potential to predict wine mouthfeel viscosity scores (or minimally to classify wines into high- and low-mouthfeel viscosity groups), as model quality was similar for the two technologies at both the calibration and cross-validation stages. Additional studies involving much larger

sample sets are needed to confirm these results, as the limited samples tested in this study ($n = 17$) did not allow for independent testing of the prediction with additional wine samples not used for model building. Once constructed, robust models based on either GC-TOF-MS or NMR data could replace sensory panels, which are expensive and time-consuming.

Additionally, interpretation of the models from a chemical standpoint has generated a list of compounds that may be directly or indirectly involved in wine mouthfeel perception. Both GC-TOF-MS and NMR PLS data and models suggest proline may be positively correlated to wine body. Although many studies report the free amino acid content of grape juices and finished wines because of their importance as nitrogen sources for yeast during fermentation and influence on the aromatic composition of wines, to date, there are no literature reports regarding the potential role of amino acids in determining wine body. Proline is one of the most abundant amino acids in grapes and has been reported at levels up to 3.7 g/L in grape must (*25*). Unlike other abundant grape amino acids (arginine, alanine, glutamate, and glutamine), proline is not used by the yeast under the anaerobic conditions of wine fermentation and remains the most abundant amino acid in the finished wine (*26*). Factors known to influence amino acid profiles in grape berries include maturity, cultivar, soil type, rootstock, temperature, season, fertilization, and crop level (*27*). If proline is a factor contributing to mouthfeel properties of wines, viticulture practices could be optimized to target desired levels.

Though proline levels may be only an indicator of another factor influencing mouthfeel, it is interesting to note that aqueous proline solutions demonstrate unusual properties for a low-molecular mass substance. With increasing concentrations, proline solutions show exponential enhancement of viscosity and increased density (*28*). ^{1}H NMR studies reveal a downfield shift of the water peak as the proline concentration increases, which is consistent with an increasing level of water structure induced by both solute−solvent and solute−solute hydrogen bonding (*29*). These studies have been conducted with aqueous solutions at concentrations at least 50-fold higher than those found in wine and need to be performed at lower concentrations in model wine solutions to determine whether these properties are relevant in a winelike matrix. Interactions between proline and other metabolites may also exhibit special properties that enhance perceived mouthfeel viscosity.

Further investigation is required to determine the connection between proline and wine body. Several observations in this study call into question the role of proline with regard to mouthfeel. Sample R02, a Riesling from New York that received one of the highest mouthfeel scores, contains almost no proline. Additionally, the absence of bins in the model from the well-isolated proline multiplet resonances centered at 1.978, 2.013, and 2.061 ppm despite the inclusion of bins 3.3925 and 3.3975, which also correspond to well-isolated proline resonances, provides conflicting evidence. These data suggest either proline does not contribute directly to wine body or more than one combination of wine chemistries that increase wine body perception exists.

The NMR model additionally identified positive correlations with spectral regions containing lactate. In the initial sensory work where organic acids were quantified by HPLC, lactate was also found to be significantly correlated to viscous mouthfeel (*6*). Lactate is present in wines primarily as a result of its conversion from malate during malolactic fermentation (*30*). In many cases, the malolactic fermentation is completed in oak barrels as opposed to stainless steel tanks, and it is possible that oak-derived compounds may also be correlated with lactate concentration and responsible for the effect on viscous mouthfeel. The negative correlation between mouthfeel score and bins corresponding to resonances for malate is also likely related to malolactic fermentation.

The GC-TOF-MS model revealed a negative correlation between fatty acids and wine body. Palmitic and stearic acids are two of the most abundant fatty acids found in grapes, and their concentration declines throughout fermentation (*31*, *32*). Yeast synthesis of fatty acids during fermentation also contributes to their levels in wines (*33*). Fatty acid concentrations in finished wine have been shown to vary with grape maturation, cultivation practices, environmental conditions, and wine production method (*34*). In the NMR-based model, negative correlation was found between perceived wine body and bins assigned to tartrate and glycerol resonances. Tartrate has not previously been identified as influencing mouthfeel properties. It is one of the major organic acids that accumulate in grapes, and its concentration is affected by cultural conditions, variety, and season (*35*). The negative correlation between glycerol and mouthfeel is difficult to interpret as other studies have shown either no correlation between glycerol content and mouthfeel in white table wines (*36*) or a variable effect that was dependent on the particular wine to which the glycerol was added (*37*).

Metabolite profiling of white wines by GC-TOF-MS and ^{1}H NMR together with PLS model construction to predict panel mouthfeel viscosity scores has been used to gain insight into the chemical basis of wine body. This exercise has generated a list of metabolites that either contribute to or are correlated with wine mouthfeel. Extensive testing of each of these metabolites in model wine solutions and in studies employing wines with large concentration ranges (naturally or by spiking with standards) is required to establish the contribution of each to perceived mouthfeel viscosity. Once key metabolites have been identified, viticultural and enological practices responsible for affecting their concentrations can be identified and implemented to tailor this wine sensory property.

ABBREVIATIONS USED

ANOVA, analysis of variance; COSY, correlation spectroscopy; GABA, γ-aminobutyric acid; GC-TOF-MS, gas chromatography-coupled time-of-flight mass spectrometry; ^{1}H NMR, proton nuclear magnetic resonance; HSQC, heteronuclear single-quantum correlation; MSTFA, *N*-methyl-*N*-(trimethylsilyl) trifluoroacetamide; PLS, partial least-squares; RMSEC, root-mean-square error of calibration; RMSEP, root-mean-square error of prediction; TMCS, trimethylchlorosilane.

ACKNOWLEDGMENT

Funding for the 600 MHz NMR instrument was provided in part by National Institutes of Health Grant RR11973.

Supporting Information Available: An example of a GC-TOF-MS chromatogram and ^{1}H NMR spectrum for a Chardonnay wine (CH02) (Figure S1) and sample mass spectral similarity searches for unknown metabolites 225846 and 224521 (Figure S2). This material is available free of charge via the Internet at http://pubs.acs.org.

LITERATURE CITED

(1) Jackson, R. S. *Wine tasting: A professional handbook*; Elsevier/Academic Press: Boston, 2002.

(2) Noble, A. C.; Bursick, G. F. The contribution of glycerol to perceived viscosity and sweetness in white wine. *Am. J. Enol. Vitic.* **1984**, *35*, 110–112.

(3) Pickering, G. J.; Heatherbell, D. A.; Vanhanen, L. P.; Barnes, M. F. The effect of ethanol concentration on the temporal perception of viscosity and density in white wine. *Am. J. Enol. Vitic.* **1998**, *49*, 306–318.
(4) Nurgel, C.; Pickering, G. Contribution of glycerol, ethanol and sugar to the perception of viscosity and density elicited by model white wines. *J. Texture Stud.* **2005**, *36*, 303–323.
(5) Gawel, R.; van Sluyter, S.; Waters, E. J. The effects of ethanol and glycerol on the body and other sensory characteristics of Riesling wines. *Aust. J. Grape Wine Res.* **2007**, *13*, 38–45.
(6) Runnebaum, R. C. Key constituents affecting wine body: An exploratory study in white table wines. M.S. Thesis, University of California, Davis, **2007**.
(7) Verhagen, J. V.; Engelen, L. The neurocognitive bases of human multimodal food perception: Sensory integration. *Neurosci. Biobehav. Rev.* **2006**, *30*, 613–650.
(8) Lindon, J. C.; Nicholson, J. K. Spectroscopic and statistical techniques for information recovery in metabonomics and metabolomics. *Annu. Rev. Anal. Chem.* **2008**, *1*, 45–69.
(9) Martin, G. J.; Guillou, C.; Martin, M. L.; Cabanis, M. T.; Tep, Y.; Aerny, J. Natural factors of isotopic fractionation and the characterization of wines. *J. Agric. Food Chem.* **1988**, *36*, 316–322.
(10) Kosir, I. J.; Kocjancic, M.; Ogrinc, N.; Kidric, J. Use of SNIF-NMR and IRMS in combination with chemometric methods for the determination of chaptalization and geographical origin of wines (the example of Slovenian wines). *Anal. Chim. Acta* **2001**, *429*, 195–206.
(11) Viggiani, L.; Morelli, M. A. C. Characterization of wines by nuclear magnetic resonance: A work study on wines from the Basilicata region in Italy. *J. Agric. Food Chem.* **2008**, *56*, 8273–8279.
(12) Pereira, G. E.; Gaudillere, J.-P.; Van Leeuwen, C.; Hilbert, G.; Lavialle, O.; Maucourt, M.; Deborde, C.; Moing, A.; Rolin, D. ^{1}H-NMR and chemometrics to characterize mature grape berries in four wine-growing areas in Bordeaux, France. *J. Agric. Food Chem.* **2005**, *53*, 6382–6389.
(13) Clark, S.; Barnett, N. W.; Adams, M.; Cook, I. B.; Dyson, G. A.; Johnston, G. Monitoring a commercial fermentation with proton nuclear magnetic resonance spectroscopy with the aid of chemometrics. *Anal. Chim. Acta* **2006**, *563*, 338–345.
(14) Gürbüz, O.; Rouseff, J. M.; Rouseff, R. Comparison of aromatic volatiles in commercial Merlot and Cabernet Sauvignon wines using GC-OF and GC-MS. *J. Agric. Food Chem.* **2006**, *54*, 3990–3996.
(15) Maggu, M.; Winz, R.; Kilmartin, P. A.; Trought, M. C. T.; Nicolau, L. Effect of skin contact and pressure on the composition of Sauvignon Blanc must. *J. Agric. Food Chem.* **2007**, *55*, 10281–10288.
(16) Joensson, S.; Hagberg, J.; van Bavel, B. Determination of 2,4,6-trichloroanisole and 2,4,6-tribromoanisole in wine using microextraction in packed syringe and gas chromatography-mass spectrometry. *J. Agric. Food Chem.* **2008**, *56*, 4962–4967.
(17) Aznar, M.; López, R.; Cacho, J.; Ferreira, V. Prediction of aged red wine aroma properties from aroma chemical composition. Partial least squares regression models. *J. Agric. Food Chem.* **2003**, *51*, 2700–2707.
(18) Lindinger, C.; Labbe, D.; Pollien, P.; Rytz, A.; Juillerat, M. A.; Yeretzian, C.; Blank, I. When Machine Tastes Coffee: Instrumental approach to predict the sensory profile of espresso coffee. *Anal. Chem.* **2008**, *80*, 1574–1581.
(19) González-Viñas, M. A.; Ballesteros, C.; Martín-Alvarez, P. J.; Cabezas, L. Relationship between sensory and instrumental measurements of texture for artisanal and industrial Manchego cheeses. *J. Sens. Stud.* **2007**, *22*, 462–476.
(20) Thybo, A. K.; Szczypiński, P. M.; Karlsson, A. H.; Dønstrup, S.; Stødkilde-Jørgensen, H. S.; Andersen, H. J. Prediction of sensory texture quality attributes of cooked potato by NMR-imaging (MRI) of raw potatoes in combination with different image analysis methods. *J. Food Eng.* **2004**, *61*, 91–100.
(21) Fiehn, O.; Wohlgemuth, G.; Scholz, M.; Kind, T.; Lee, D. Y.; Lu, Y.; Moon, S.; Nikolau, B. Quality control for plant metabolomics: Reporting MSI-compliant studies. *Plant J.* **2008**, *53*, 691–704.
(22) Fiehn, O.; Wohlgemuth, G.; Scholz, M. Setup and annotation of metabolomic experiments by integrating biological and MS metadata. *Proc. Lect. Notes Bioinf.* **2005**, *3615*, 224–239.
(23) Cui, Q.; Lewis, I. A.; Hegeman, A. D.; Anderson, M. E.; Li, J.; Schulte, C. F.; Westler, W. M.; Eghbalnia, H. R.; Sussman, M. R.; Markley, J. L. Metabolite identification via the Madison Metabolomics Consortium Database. *Nat. Biotechnol.* **2008**, *26*, 162–164.
(24) Martens, H.; Martens, M. Modified Jack-knife estimation of parameter uncertainty in bilinear modeling by partial least squares regression (PLSR). *Food Qual. Prefer.* **2000**, *11*, 5–16.
(25) Huang, Z.; Ough, C. S. Amino acid profiles of commercial grape juices and wines. *Am. J. Enol. Vitic.* **1991**, *42*, 261–267.
(26) Lehtonen, P. Determination of amines and amino acids in wine: A review. *Am. J. Enol. Vitic.* **1996**, *47*, 127–133.
(27) Stines, A. P.; Grubb, J.; Gockowiak, H.; Henschke, P. A.; Høj, P. B.; van Heeswijick, R. Proline and arginine accumulation in developing berries of *Vitis vinifera* L. in Australian vineyards: Influence of vine cultivar, berry maturity and tissue type. *Aust. J. Grape Wine Res.* **2000**, *6*, 150–158.
(28) Schobert, B.; Tschesche, H. Unusual solution properties of proline and its interactions with proteins. *Biochim. Biophys. Acta* **1978**, *541*, 270–277.
(29) Civera, M.; Sironit, M.; Fornili, S. L. Unusual properties of aqueous solutions of L-proline: A molecular dynamics study. *Chem. Phys. Lett.* **2005**, *415*, 274–278.
(30) Boulton, R. B.; Singleton, V. L.; Bisson, L. F.; Kunkee, R. E. *Principles and Practices of Winemaking*; Aspen Publishers, Inc.: Gaithersburg, MD, 1998.
(31) Gallander, J. F.; Peng, A. C. Lipid and fatty acid compositions of different grape types. *Am. J. Enol. Vitic.* **1980**, *31*, 24–27.
(32) Ancin, C.; Ayestaran, B.; Garcia, A.; Garrido, J. Evolution of fatty acid contents in Garnacha and Viura musts during fermentation and the aging of wine. *Z. Lebensm.-Unters. -Forsch. A* **1998**, *206*, 143–147.
(33) Nykanen, L. Formation and occurrence of flavor compounds in wine and distilled alcoholic beverages. *Am. J. Enol. Vitic.* **1986**, *37*, 84–96.
(34) Yunoki, K.; Yasui, Y.; Hirose, S.; Ohnishi, M. Fatty acids in must prepared from 11 grapes grown in Japan: Comparison with wine and effect on acid ethyl ester formation. *Lipids* **2005**, *40*, 361–367.
(35) Kliewer, W. M.; Howarth, L.; Omori, M. Concentrations of tartaric acid and malic acids and their salts in *Vitis vinifera* grapes. *Am. J. Enol. Vitic.* **1967**, *18*, 42–54.
(36) Noble, A. C.; Bursick, G. F. The contribution of glycerol to perceived viscosity and sweetness in white wine. *Am. J. Enol. Vitic.* **1984**, *35*, 110–112.
(37) Gawel, R.; van Sluyter, S.; Waters, E. J. The effects of ethanol and glycerol on the body and other sensory characteristics of Riesling wines. *Aust. J. Grape Wine Res.* **2007**, *13*, 38–45.

Received June 5, 2009. Accepted June 20, 2009.